LAND DEGRADATION & DEVELOPMENT
Land Degrad. Develop. (2017)
Published online in Wiley Online Library (wileyonlinelibrary.com) **DOI**: 10.1002/ldr.2812

PYROGENIC CARBON CONTRIBUTES SUBSTANTIALLY TO CARBON STORAGE IN INTACT AND DEGRADED NORTHERN PEATLANDS

Jens Leifeld[1]*, Christine Alewell[2], Cédric Bader[1], Jan Paul Krüger[2,3], Carsten W. Mueller[4], Michael Sommer[5], Markus Steffens[4], Sönke Szidat[6]

[1]*Agroscope, Climate/Air Pollution Group, Reckenholzstrasse 191, CH-8046 Zurich, Switzerland*
[2]*Departement Umweltgeowissenschaften, Universität Basel, Bernoullistrasse 30, CH-4056 Basel, Switzerland*
[3]*UDATA GmbH – Umwelt und Bildung, Hindeburgstr. 1, D-67433 Neustadt/Wstr, Germany*
[4]*Technische Universität München, Lehrstuhl für Bodenkunde, Emil-Ramann Strasse 2, D-85354 Freising, Germany*
[5]*Leibniz-Zentrum für Agrarlandschaftsforschung (ZALF) e.V, Institut für Bodenlandschaftsforschung, Eberswalder Str. 84, D-15374 Müncheberg, Germany*
[6]*Departement für Chemie und Biochemie, Labor zur Analyse von Radiokohlenstoff mit AMS (LARA), Universität Bern & Oeschger Centre for Climate Change Research, Freiestrasse 3, CH-3012 Bern, Switzerland*

Received 30 September 2016; Revised 17 August 2017; Accepted 31 August 2017

ABSTRACT

Pyrogenic carbon (PyC) derives from incomplete combustion of organic matter and is ubiquitous in terrestrial and aquatic systems. Most PyC is inherently more stable against decomposition than plant residues, and PyC therefore forms an important component of the global carbon (C) cycle. During the Holocene, about 436 Pg organic C accumulated in northern peatlands, and we hypothesize that PyC may contribute substantially to that C stock. We studied 70 samples from 19 intact and degraded European peatland sites and analyzed their PyC content by ^{13}C nuclear magnetic resonance spectroscopy and molecular modeling and peat age and accumulation by radiocarbon dating. Classification of a peatland as either intact or degraded was based on the comparison between apparent and expected long-term C accumulation rates. On average, PyC amounted for 13·5% of soil C across sites, and accounted for up to 50% at single sites. The amount of PyC increased significantly with peat age. Degraded peatlands had lost approximately 56 kg C m^{-2}, half of their former C stock. However, degraded peat had higher PyC contents than intact one. Selective enrichment of PyC during both peat build-up and decomposition seems to be an important factor fostering PyC accumulation. Assignment of our results to peatlands of the northern hemisphere, stratified by age, revealed an estimated PyC stock of 62 (±22) Pg. Our estimate indicates a substantial and hitherto unquantified contribution of northern peatlands to global PyC storage. © 2017 The Authors. Land Degradation & Development Published by John Wiley & Sons Ltd.

KEY WORDS: organic soil; pyrogenic carbon; soil degradation; radiocarbon; NMR spectroscopy

INTRODUCTION

Fire is present in the Earth system since the appearance of terrestrial plants on the continents. It is a property of many natural ecosystems but important also when humans convert forests to agricultural land (Bowman *et al*., 2009). Fire is therefore considered the most ancient land management tool that shaped landscapes for thousands of years (Santín & Doerr, 2016). Black or pyrogenic carbon (PyC) naturally originates from vegetation fires via incomplete combustion of organic material, forming charcoal, tar or soot. These compounds are of different composition and stability and part of a combustion continuum (Hedges *et al.,* 2000). PyC is abundant in many soils and can make up a significant share of total soil organic carbon (SOC). In mineral soil, PyC may account for around 5–15% of SOC (Druffel, 2004; Hockaday *et al.,* 2007), although in some soils that are altered by human influence, PyC might constitute up to 60% of SOC (Glaser *et al.,* 2002; Skjemstad *et al.,* 2002; Lehmann *et al.,* 2008). The global rate of PyC entering soil, mostly from biomass burning, is approximately 0·056–0·137 Pg C $year^{-1}$ (Bird *et al.,* 2015), a small amount compared with annual soil C inputs from net primary production (NPP) of approx. 60 Pg C (Janzen, 2004). According to different estimates, PyC in soil globally accounts for 71–212 Pg (Santín *et al.,* 2016), 54–109 Pg (Bird *et al.,* 2015) or ca 200 Pg (Reisser *et al.,* 2016) of a global total of 1,500 to 3,000 Pg SOC (Scharlemann *et al.,* 2014). PyC stocks in soil are large relative to PyC formation rates, speaking for a high relative resistance to microbial decomposition (Santín *et al.,* 2016). Occurrence of organic matter moieties similar to PyC have also been attributed to *in situ* formation via photo-oxidation (Hartman *et al.,* 2015), but we consider this process more relevant in surface waters regularly exposed to radiation.

About 550 Pg of the global SOC stock is located in organic soils, most of it in northern peatlands (Yu *et al.,* 2010). Vegetation and peat fires recurrently occur in natural peatlands with frequencies in the order of decades to a few centuries (Pitkänen & Grönlund, 2001; Franzen & Malmgren, 2012). Such fires not only produce end members of complete redox reactions, that is, CO_2 and H_2O, but smoke compounds such as reduced organic volatiles that impair human health (Konovalov *et al*., 2011), as well as

*Correspondence to: J. Leifeld, Agroscope, Climate/Air Pollution Group, Reckenholzstrasse 191, CH-8046 Zurich, Switzerland.
E-mail: jens.leifeld@agroscope.admin.ch

charcoal, soot and tar. The latter products are indicative for incomplete and partially smoldering combustion and result in formation of discrete charcoal layers in peatlands (Yokelson *et al.,* 1997; Sillasoo *et al.,* 2011). Further, smoldering combustion changes peat chemistry towards a higher proportion of aromatic moieties and a preferential loss of oxygen containing functional groups such as polysaccharides (Zaccone *et al.,* 2014). Fire recurrence and hence PyC formation in peatlands has already been influenced historically by human activity such as slash and burn practices in Northern Europe (Tolonen, 1985) and by agropastoral activities in Neolithic Central Europe (Rius *et al.,* 2009). The contemporary increase in global peatland drainage in conjunction with a changing climate may affect frequency and force of peatland fires substantially. Turetsky *et al*. (2015) elaborated that peat, under undisturbed conditions, is hydrologically protected from deep peat fires; that is, mostly the vegetation and uppermost peat layers (<0·2 m) ignite in case of lightning. Likelihood for ignition as well as occurrence and severity of smoldering combustion will become higher at peat moisture contents of <125% dry weight (Rein *et al.,* 2008). After drainage, declining moisture may enable smoldering combustion down to deeper layers. In drained tropical peatland, recurrent fires at the same site consume between 23 and 206 t dry peat ha^{-1} and burn the peat down to 0·4 m depth (Konecny *et al.,* 2016).

The high recalcitrance inherent to some forms of PyC (Liang *et al.,* 2008; Woolf & Lehmann, 2012; Hardy *et al.,* 2017) may be even more important under conditions of permanent waterlogging as typical for intact peat bogs, where oxygen scarcity limits organic matter breakdown (Clymo *et al.,* 1998). This may cause selective enrichment of PyC in organic soils. In paddy fields, which are at least temporarily anaerobic, charcoal may be stored for several thousand years (Wu *et al.,* 2015). Yet despite a presumably important role of PyC for peatland C storage, no comprehensive estimate of PyC contents exists for peatlands that goes beyond qualitative methods such as charcoal counting or quantification at the scale of few single sites (Reisser *et al.,* 2016).

Globally, about 10% of the peatlands are altered by humans for agriculture or forestry, with a share of >90% in some European countries (Joosten, 2010). Through land use change and peatland drainage, peat becomes aerated and is decomposed, causing high greenhouse gas fluxes, mostly as CO_2 (Kasimir-Klemedtsson *et al.,* 1997). Given the frequency of charcoal found in intact peatlands and its recalcitrance (Franzen & Malmgren, 2012), we suppose that upon drainage and peat oxidation, PyC becomes selectively enriched owing to preferential utilization of more labile C moieties.

Here, we study a large set of peat samples from various locations to (i) quantify their PyC content, (ii) address the relationship between PyC content and peat degradation state and age and (iii) estimate the overall amount of PyC that has accumulated in northern peatlands during the Holocene.

MATERIAL AND METHODS

We analyzed a data set of 70 peat samples, representing 19 sites from Finland, Germany and Switzerland, for their chemical composition by elemental analysis and solid state ^{13}C nuclear magnetic resonance (NMR) spectroscopy and a subsample of 54 samples for their ^{14}C age. The sites represented the full range of peatland states from intact, peat-forming bogs and fens to strongly degraded, earthified peat of intensively managed agricultural sites after decadal to centennial drainage. Further, we assigned our PyC measurements in organic soil to a data set of the peatland area, C stock and peat age distribution in the whole northern hemisphere (Loisel *et al.,* 2014) to obtain an estimate of northern peatland PyC.

Sites

Sampling sites comprise temperate and boreal climate as well as the land use types forest, grassland, cropland and natural land (i.e., intact mire). Depending on site conditions and remaining peat depth, samples were taken down to a maximum of 2 m. In all cases, we used peatland corers and took volumetric samples that allow for measuring both, soil mass and elemental contents. Land use was classified during site visits. Land use types cropland, grassland and forest are assigned to sites that are drained and managed; that is, forests are planted and not peat forming. Grasslands are used for haymaking/cutting, grazing or both. Natural land refers to intact mires with peat forming vegetation as surveyed during site visits. At all managed sites, drainage onset dates back many decades ago. Drainage depths differ but is in most cases >0·5 m. Table I gives an overview of the 19 sampling sites, their land use, sampling depths, PyC content, measured ^{14}C signatures and assigned ages.

^{14}C Measurement and Age Calibration

$F^{14}C$ values were measured for 54 bulk peat samples at the Laboratory for the Analysis of Radiocarbon with accelerator mass spectrometer (LARA) at University of Bern (Szidat *et al.,* 2014). Calibrated ^{14}C ages were determined with OxCal 4·2 (Ramsey, 2009) using the IntCal13 data set (Reimer *et al.,* 2013) with the NH1 extension (Hua *et al.,* 2013) and presented as years before 2016. When multiple samples from the same core were analyzed, we added the criterion that uppermost samples always were younger than deeper samples. Nine samples with modern radiocarbon signature (i.e., $F^{14}C > 1{\cdot}0$) may be attributed to two different ages, corresponding to either of the two slopes of the bomb peak. In case of sites Gruyere, Lakkasuo and Seebodenalp, the radiocarbon signature of the uppermost samples was still below that of the contemporary atmosphere (at time of sampling); therefore, the higher calibrated age was assigned to these samples. For sites Eigenried and Hagenmoss, choice was based on whether the calculated C accumulation rates above the youngest sample were close to that of the deeper, unambiguously age-dated samples. For site Ahlen-Falkenberg, the data were not suited to assign the older or the younger age

Table I. Overview of sites and samples

Sample ID	Site	Subsite	Sampling depth (cm)	Coordinates	Land-use	% PyC	$F^{14}C$ ± uncertainty (1σ)		Mean age (years before 2016)	Degradation state
1	Eigenried	Eigenried	122	47·09°N, 4·58°E	N	9·1	N.A.		N.A.	N.A.
2	Eigenried	Eigenried	14	47·09°N, 4·58°E	N	1·4	0·975	±0·002	116	I
3	Eigenried	Eigenried	182	47·09°N, 4·58°E	N	14·2	0·696	±0·002	3206	I
4	Eigenried	Eigenried	5	47·09°N, 4·58°E	N	3.7	1·101	±0·003	21	I
5	Eigenried	Eigenried	38	47·09°N, 4·58°E	N	7·1	0·926	±0·005	669	I
6	Eigenried	Eigenried	62	47·09°N, 4·58°E	N	6·6	0·860	±0·002	1,290	I
7	Ahlen-Falkenberg	Extensiv_1	81	53·41°N, 8·49°E	GL	7·1	0·796	±0·004	1,849	I
8	Ahlen-Falkenberg	Extensiv_2	9	53·41°N, 8·49°E	GL	6·6	0·939	±0·005	595	D
9	Ahlen-Falkenberg	Intensiv_1	81	53·41°N, 8·49°E	GL	9·2	0·763	±0·004	2,252	I
10	Ahlen-Falkenberg	Intensiv_2	25	53·41°N, 8·49°E	GL	2·4	0·821	±0·004	1,538	D
11	Ahlen-Falkenberg	Intensiv_2	81	53·41°N, 8·49°E	GL	4·2	0·755	±0·004	2,282	I
12	Gruyere	Gruyere	13	47·24°N, 7·05°E	N	0.2	0·997	±0·003	62	I
13	Gruyere	Gruyere	17	47·24°N, 7·05°E	N	0.1	1·016	±0·002	61	I
14	Gruyere	Gruyere	188	47·24°N, 7·05°E	N	5·7	0·591	±0·002	4,917	I
15	Gruyere	Gruyere	194	47·24°N, 7·05°E	N	7·7	0·586	±0·002	4,979	I
16	Gruyere	Gruyere	23	47·24°N, 7·05°E	N	3·3	1·001	±0·002	116	I
17	Gruyere	Gruyere	83	47·24°N, 7·05°E	N	10·7	0·817	±0·002	1,641	I
18	Hagenmoos	Hagenmoos	113	47·24°N, 8·52°E	FL	11·4	0·391	±0·001	8,469	D
19	Hagenmoos	Hagenmoos	164	47·24°N, 8·52°E	FL	10·7	0·334	±0·001	10,101	D
20	Hagenmoos	Hagenmoos	182	47·24°N, 8·52°E	FL	19·5	0·287	±0·001	11,769	D
21	Hagenmoos	Hagenmoos	35	47·24°N, 8·52°E	FL	3·4	1·294	±0·003	56	I
22	Hagenmoos	Hagenmoos	5	47·24°N, 8·52°E	FL	9·1	N.A.		N.A.	N.A.
23	Hagenmoos	Hagenmoos	53	47·24°N, 8·52°E	FL	10.2	0·702	±0·002	3,086	D
24	Lakkasuo	minerotrophic natural_2	49	61·80°N, 24·32°E	N	9·4	0·907	±0·005	772	I
25	Lakkasuo	minerotrophic natural_3	49	61·80°N, 24·32°E	N	10.0	0·902	±0·005	795	I
26	Lakkasuo	ombrotrophic drained_1	49	61·80°N, 24·32°E	FL	7·1	0·985	±0·005	210	I
27	Lakkasuo	ombrotrophic drained_2	49	61·80°N, 24·32°E	FL	0.2	0·957	±0·005	470	I
28	Lakkasuo	ombrotrophic natural_2	49	61·80°N, 24·32°E	N	1·8	1·005	±0·005	151	I
29	Paulinenaue	Mais_a	2	52·69°N, 12·72°E	CL	11·5	N.A.		N.A.	N.A.
30	Paulinenaue	Mais_a	8	52·69°N, 12·72°E	CL	9·9	0·870	±0·004	1,087	D
31	Paulinenaue	Mais_a	86		CL	12·0	0·653	±0·003	N.A.	I

(*Continues*)

Table I. (Continued)

Sample ID	Site	Subsite	Sampling depth (cm)	Coordinates	Land-use	% PyC	$F^{14}C$ ± uncertainty (1σ)		Mean age (years before 2016)	Degradation state
				52·69°N, 12·72°E						
32	Paulinenaue	Mais_d	2	52·69°N, 12·72°E	CL	16.0	N.A.		N.A.	N.A.
33	Paulinenaue	Mais_d	55	52·69°N, 12·72°E	CL	10.1	N.A.		N.A.	N.A.
34	Ahlen-Falkenberg	Naturnah_1	9	53·41°N, 8·49°E	N	2.0	1·165	±0·006	42	I
35	Ahlen-Falkenberg	Naturnah_2	9	53·41°N, 8·49°E	N	1·9	1·084	±0·005	37	I
36	Ahlen-Falkenberg	Naturnah_3	9	53·41°N, 8·49°E	N	0·6	1·139	±0·006	42	I
37	Paulinenaue	P1_b	2	52·69°N, 12·72°E	GL	7·5	N.A.		N.A.	N.A.
38	Paulinenaue	P1_b	43	52·69°N, 12·72° E	GL	21·7	N.A.		N.A.	N.A.
39	Paulinenaue	P247_d	2	52·69°N, 12·72°E	GL	10·9	N.A.		N.A.	N.A.
40	Paulinenaue	P247_d	26	52·69°N, 12·72°E	GL	11·1	N.A.		N.A.	N.A.
41	Paulinenaue	P247_d	49	52·69°N, 12·72°E	GL	10·6	N.A.		N.A.	N.A.
42	Paulinenaue	P247_d	61	52·69°N, 12·72°E	GL	40·9	0·535	±0·003	5,844	D
43	Paulinenaue	P247_d	8	52·69°N, 12·72°E	GL	13·4	0·683	±0·003	3,337	D
44	Paulinenaue	P247_d	85	52·69°N, 12·72°E	GL	19·7	0·352	±0·002	9,463	D
45	Paulinenaue	P346_d	2	52·69°N, 12·72°E	GL	9·5	N.A.		N.A.	N.A.
46	Paulinenaue	P346_d	8	52·69°N, 12·72°E	GL	11·4	0·847	±0·004	1,331	D
47	Paulinenaue	P346_d	85	52·69°N, 12·72°E	GL	19·1	0·376	±0·002	8,729	D
48	Paulinenaue	P4_a	2	52·69°N, 12·72°E	GL	9·4	N.A.		N.A.	N.A.
49	Paulinenaue	P4_a	37	52·69°N, 12·72°E	GL	24·1	0·717	±0·004	2,869	D
50	Paulinenaue	P4_a	46	52·69°N, 12·72°E	GL	27·9	0·487	±0·002	6,630	D
51	Paulinenaue	P4_a	49	52·69°N, 12·72°E	GL	25·2	0·594	±0·003	4,743	D
52	Paulinenaue	P4_a	8	52·69°N, 12·72°E	GL	11·8	0·845	±0·004	1,349	D
53	Paulinenaue	P4_a	84	52·69°N, 12·72°E	GL	15·6	0·328	±0·002	10,138	D
54	Paulinenaue	P4_b	2	52·69°N, 12·72°E	GL	10.5	N.A.		N.A.	N.A.
55	Paulinenaue	P4_b	40	52·69°N, 12·72°E	GL	35·7	0·579	±0·003	5,022	D
56	Paulinenaue	P4_b	46	52·69°N, 12·72°E	GL	49·1	0·438	±0·002	7,576	D
57	Paulinenaue	P4_b	52	52·69°N, 12·72°E	GL	22·5	0·472	±0·003	6,940	D
58	Paulinenaue	P4_b	76	52·69°N, 12·72°E	GL	13.7	N.A.		N.A.	N.A.
59	Paulinenaue	P4_b	42	52·69°N, 12·72°E	GL	52·2	0·491	±0·003	6,589	D
60	Witzwil	P33_c	135	46·98°N, 7·05°E	CL	16·6	0·307	±0·002	10,795	D
61	Witzwil	P33_a	10		CL	19·6	0·631	±0·003	4,107	D

(*Continues*)

Table I. (Continued)

Sample ID	Site	Subsite	Sampling depth (cm)	Coordinates	Land-use	% PyC	$F^{14}C$ ± uncertainty (1σ)		Mean age (years before 2016)	Degradation state
				46·98°N, 7·05°E						
62	Witzwil	P33_a	50	46·98°N, 7·05°E	CL	12·4	0·407	±0·002	8,128	D
63	Witzwil	Spring_c	50	46·98°N, 7·05°E	CL	6.1	0·390	±0·002	8,445	D
64	Seebodenalp	SBAb	2	47·06°N, 8·46°E	GL	5·9	0·991	±0·002	170	I
65	Seebodenalp	SBAb	22	47·06°N, 8·46°E	GL	10.0	0·820	±0·002	1,633	D
66	Seebodenalp	SBAa	34	47·06°N, 8·46°E	N	12·7	0·738	±0·002	2,634	D
67	Seebodenalp	SBAa	2	47·06°N, 8·46°E	N	7·1	1.003	±0·002	116	I
68	Witzwil	Staatswald1	88	46·98°N, 7·05°E	FL	11·8	0·433	±0·002	7,651	D
69	Witzwil	Witzwil B	3	46·98°N, 7·05°E	CL	19·3	N.A.		N.A.	N.A.
70	Witzwil	Witzwil B	24	46·98°N, 7·05°E	CL	21·3	N.A.		N.A.	N.A.

CL, cropland; GL, grassland; FL, forest; N, natural; I, intact, D, degraded; N.A., not applicable.

and the reported age represents the mean and range for both possibilities.

Assignment of Sites as Intact or Degraded

Soil organic carbon stocks above age-dated peat layers were used to infer SOC accumulation rates. These rates were compared to a global data set of Loisel *et al.* (2014) in order to distinguish between sites that resemble typical accumulation rates and those that apparently accumulated little.

In intact peatlands, age–carbon relationships give precise estimates on long-term rates of net C accumulation (LORCA) (Belyea & Malmer, 2004). In degrading peatlands, this approach underestimates the true average accumulation that occurred since peatland onset but before drainage because of oxidation of a substantial fraction of the former peat deposit since land use change. We refer here to this estimate as apparent C accumulation. We inferred the fraction of C lost by comparing the apparent C accumulation with the grand mean of SOC accumulation in peatlands of the northern hemisphere (Loisel *et al.,* 2014). We classified our peatlands as 'degraded' when their apparent C accumulation rate was below the minimum expected value from Loisel *et al.* (2014) (i.e., their lower confidence interval of 18·9 g C m^{-2} y^{-1}) and as 'intact' when the apparent C accumulation rate was above the expected minimum. Hence, our classification solely takes C dynamics into account. We consider our classification as generic because LORCA at individual sites may well deviate from the grand mean owing to differences in environmental conditions upon peat formation.

NMR Spectroscopy and PyC Quantification

Cross polarization magic angle spinning ^{13}C NMR spectroscopy was accomplished with a Bruker DSX 200 spectrometer (Bruker BioSpin GmbH, Karlsruhe, Germany) at the Lehrstuhl für Bodenkunde, TU München, Germany. Finely ground and homogenized bulk peat samples were filled into zirconium dioxide rotors and spun in a magic angle spinning probe at a rotation speed of 5 kHz to minimize chemical anisotropy. A ramped ^{1}H pulse was used during a contact time of 1 ms to prevent Hartmann–Hahn mismatches. The delay time was set to 1 s. Chemical shifts were referenced to tetramethylsilane (TMS = 0 ppm). For application to the molecular mixing model, the single chemical shift regions were integrated as follows: alkyl C (0 to 45 ppm), O/N-alkyl C (45 to 110 ppm), aryl/olefine C (110 to 165 ppm) and carbonyl/carboxyl/amide C (165 to 210 ppm). For samples rich in PyC, the integrated area of spinning side bands derived from the aryl C main signal were added to aryl C.

We quantified PyC by using NMR and elemental data (C, H, N and O) with a linear molecular mixing model (Baldock *et al.,* 2004) (Figure S1). The mixing model assigns virtual spectra of pure compound classes to the measured sample and adjusts the share of each compound class by minimizing the error. It uses the NMR and elemental data. For a statistical evaluation of NMR data, spectra were integrated with higher resolution to obtain seven spectral regions (see Figure S2). A principal component analysis was run on all ^{14}C–dated samples with those seven major NMR spectral regions (−10–45, 45–60, 60–90, 90–110, 110–145, 145–165 and 165–210 ppm) and elemental data (SOC content, atomic ratios N/C, H/C, O/C) as input data. The NMR regions were not the same as those used for the molecular mixing model in order to make better use of the spectral information. The cross polarization magic angle spinning technique may underestimate condensed forms of PyC and, in combination

with the molecular mixing model, be a measure of less condensed aromatic structures (Kane *et al.,* 2010). We therefore consider our PyC estimates as conservative. Further, we believe the method is specific for identifying PyC. Aromatic moieties in ^{13}C NMR spectra from peat may also be associated with kerogen (Smernik *et al.,* 2006). The relationship of alkyl-C with depth and age as well as the van Krevelen plot and SEM images of some of the samples, however, underline that formation of kerogen does not play a major role for the studied sites (see Figures S3 and S4 and corresponding text).

Elemental Analysis

Contents of C, H and N were measured in an elemental analyzer (Hekatech, Germany) by dry combustion at 1,400 °C, gas chromatography separation and thermal conductivity detector detection. Oxygen was measured as CO after pyrolysis at 1,000 °C with the same instrument. Samples containing carbonate were pre-treated using acid fumigation with 0·5 M HCl in a desiccator overnight.

Statistics

We tested for differences in chemical composition between intact and degraded peat (NMR and elemental composition) by *t*-test after square root transformation of data. We used linear regression to infer the relationship between peat age, peat C stock and PyC content and give mean values and, in brackets, one standard error of the mean or, correspondingly, the regression coefficients, in the text.

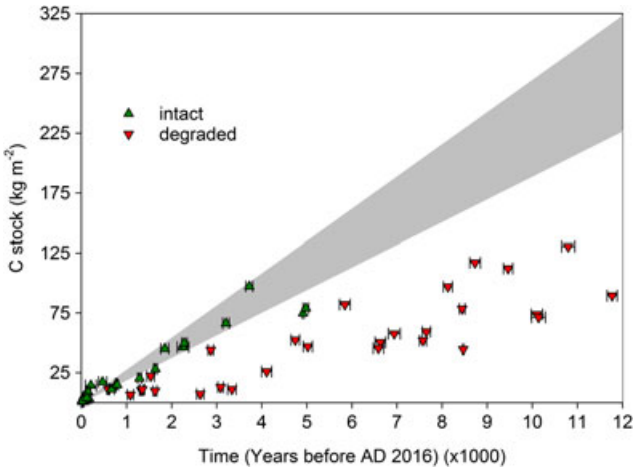

Figure 1. Peatland soil C accumulation during the Holocene. The grey area indicates the upper and lower 95% confidence interval (CI) of predicted C accumulation in northern peatlands (Loisel *et al.,* 2014). Data points represent C stocks of ^{14}C-dated peat layers from this study. Sites were classified as intact (n = 26) if their accumulation rate was situated within the prediction of Loisel *et al.* (2014) and as degraded, if their accumulation rate was situated below (n = 28). Their distance to the lower CI gives the minimum amount of soil C lost upon cultivation. Horizontal error bars represent the lower and the upper range of the 68% CI of calibrated radiocarbon dates. 'Intact' outside the gray area are data from the bog gruyere that accumulated C at 15·4 g C m^{-2} y^{-1} and thus at a rate lower than the lower CI in Loisel *et al.* (2014) (18·9 g C m^{-2} y^{-1}). [Colour figure can be viewed at wileyonlinelibrary.com]

PyC Stocks in Northern Hemisphere Peatlands

Loisel and co-authors (Loisel *et al.,* 2014) presented a comprehensive estimate on Holocene C accumulation and storage in the peatlands of the northern hemisphere. Their data set includes calibrated peatland inception ages, their distribution and mean C accumulation rates for 500-year bins during the Holocene. We weighted every of their 500-year bins of peat inception by its corresponding mean rate of C accumulation to obtain the actual mean age of the whole peat profile for any particular peat inception age. The age classes were then multiplied with their relative frequency as reported by Loisel *et al.* (2014) to obtain a weighed distribution of peat ages in the northern hemisphere. We then applied the regression equation from our Figure 3 to each of the age classes to infer PyC stocks. We accounted for uncertainty by using upper and lower confidence limits of our regression for calculating PyC content for any of the age classes separately.

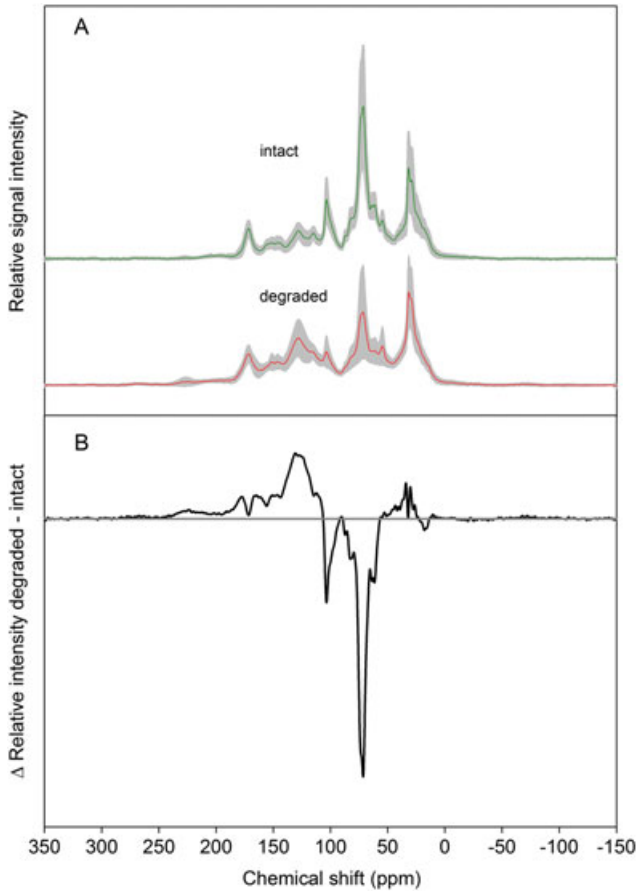

Figure 2. Peat composition revealed by nuclear magnetic resonance spectroscopy. Panel a shows the average (±1 standard deviation) cross polarization magic angle spinning ^{13}C nuclear magnetic resonance spectrum for intact and degraded peat. The differential spectrum (panel b) reveals a preferential loss of O-alkyl C (signals at around 72 and 105 ppm) and a selective enrichment of both aliphatic (signal around 30 ppm) and aromatic (130 ppm) C in old peat from drained organic soils relative to intact peats. [Colour figure can be viewed at wileyonlinelibrary.com]

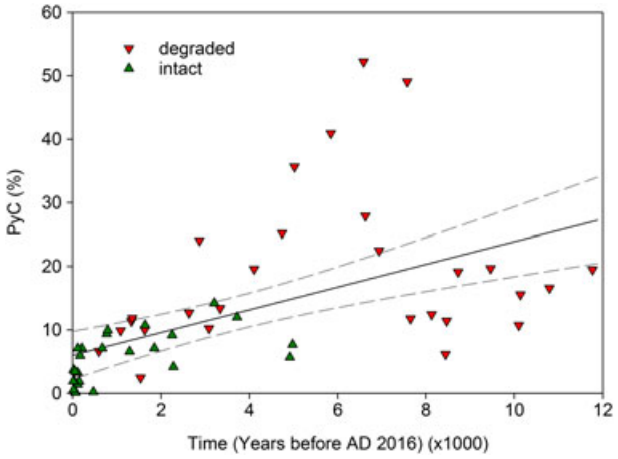

Figure 3. Percentage of pyrogenic carbon in soil organic carbon as a function of peat age in intact (n = 26) and degraded (n = 28) peatlands. Across all 54 dated samples, percentage of PyC increased significantly by 1·8% (±0·4; $p < 0·001$) per millennium. The offset is 6·0% (±1·9). Lines are regressions (solid) and their 95% confidence intervals (dashed) for all 54 data points. [Colour figure can be viewed at wileyonlinelibrary.com]

RESULTS AND DISCUSSION

Our approach to distinguish peatland sites into intact and degraded ones by means of their C accumulation rate revealed sharp differences between those two groups and across sites. Twenty-six of our dated samples were classified as intact, with an average LORCA of 36·9 (±6·1) g C m^{-2} y^{-1}, whereas the apparent C accumulation rate at degraded sites (n = 28) was only 9·0 (±0·7) g C m^{-2} y^{-1}. The majority of the sites identified as 'natural' with respect to their state in the field were classified as 'intact' with the selected radiocarbon approach (18 of 26), whereas almost all of those identified as 'managed' in the field classified as 'degraded' (27 of 28, Table I). There were, however, managed sites with apparent C accumulation rates still inside the uncertainty range of the grand mean, suggesting that those soils, particularly in deeper layers, are not yet strongly affected by drainage and peat loss. This was specific to sites with only extensive management or shallow drainage. Relative to their expected minimum C accumulation of 18·9 g C m^{-2} y^{-1} (Loisel *et al.,* 2014), degraded sites lost on average 52% or, correspondingly, 55·6 (±7·0) kg C m^{-2}. We consider this loss as substantial, given that intact peatlands store approximately 100 kg C m^{-2} (Joosten, 2010), and as indicative of the situation of many peatlands in Europe with its long history of peatland drainage and management. Our carbon loss estimate is conservative given that it is based on the distance between apparent accumulation and the lower confidence interval of the accumulation measured for intact peatlands.

Although sampling depths varied widely between 0·02 and 1·97 m (Table I), the average depth was very similar for both classes (degraded 0·57 ± 0·09 m, intact 0·56 ± 0·11 m). Degraded peat was on average much older (5,735 ± 640 years) than intact peat (1,153 ± 300 years) (Figure 1). This difference mirrors the substantial loss of young peat since drainage onset, leaving behind topsoil peat that is older than that at intact sites (Krüger *et al.,* 2016). The loss of younger material, in conjunction with higher bulk densities when sites were managed, resulted in a steeper slope and a larger offset of age-depth curves (Figure S5). In our data set, degraded and intact peat differed significantly in composition. Degraded peat had higher atomic N/C ratios (0·042 ± 0·003) than intact peat (0·029 ± 0·002) but lower H/C (1·29 ± 0·03 vs. 1·42 ± 0·02) and O/C ratios (0·52 ± 0·02 vs. 0·56 ± 0·02) and contained less organic C (39·5 ± 2·5% vs. 49·5 ± 1·0%). Further, degraded peat was richer in aryl C and alkyl C, whereas it contained much less O-alkyl C than intact peat (Figure 2). A principal component analysis of NMR and elemental data revealed that the drainage state (intact vs. degraded) was a meta-driver for peat organic matter chemistry (Figure S1). Thus, the chosen criterion in Figure 1 to distinguish degraded versus intact sites by means of the ^{14}C-derived accumulation rate was selective also for peat chemistry. Peat chemical composition typically changes down the peat profile towards a depletion of oxygen-containing moieties and an enrichment of non-oxygenated aliphatic and aromatic compounds (Leifeld *et al.,* 2012; Biester *et al.,* 2014). We therefore presumed that differences in C, H, O and NMR signatures for intact versus degraded sites partially reflect different peat ages – older and more recalcitrant peat is exposed closer to the surface at degraded than at intact sites. Further, wide N/C ratios are typical for degraded peatlands owing to N input from agricultural management and selective enrichment of N during peat decomposition (Berglund *et al.,* 2010; Krüger *et al.,* 2015).

For the whole data set (n = 70), PyC averaged 13·5% (±1·2) of SOC. This value is almost exactly the same as recently reported in a global review for, mostly, mineral soils (13·7%, Reisser *et al.,* 2016). PyC increased significantly with peat age by 1·8% (±0·4) per millennium across all dated samples (Figure 3). PyC/SOC ratios also increased significantly when only intact sites were considered (p = 0·02), indicating PyC formation and accumulation during peat build-up. Single profiles revealed trends towards increasing PyC/SOC ratios with age as well (Figure and Table S1), although these trends were, possibly owing to the small number of samples studied per site, not significant. Still, trends were always positive, supporting our hypothesis that PyC enrichment over time is a common phenomenon in organic soils. Figure S6 also shows that PyC accumulation was highly site specific, denoting differences in peatland type, hydrology, climate and thus fire recurrence and properties. Carbon stored in degraded peat contained significantly ($p < 0·001$) more PyC (18·9 ± 2·4%) than C stored in intact peat (5·5 ± 0·8%). The higher PyC share in degraded peat corresponds to differences in elemental composition of organic matter shown above and is in line with an increase in N and C relative to H and O upon formation of charred compounds when peat burns (Zaccone *et al.,* 2014). These may encompass synthesis of heterocyclic N forms such as

pyrrole and indole upon heating of the peat (Almendros *et al.,* 2003). When we compared only peatlands with an overlapping age range (600 to 5,000 years), degraded peats of that age still had higher PyC/SOC ratios than intact peats of the same age (13·1 ± 1·9 vs. 8·7 ± 0·8%, $p = 0{\cdot}046$). However, PyC/SOC ratios did not increase with age at degraded sites ($p = 0{\cdot}25$).

We see three possible mechanisms explaining PyC increase with peat age and hence soil depth in our data: selective enrichment, downward transport and changing fire frequencies. First, peat formation goes along with a respiratory loss of up to 90% of the NPP before assimilates enter the deeper peat zone, where anoxic conditions slow down decomposition (Clymo, 1984). As a result, the proportion of NPP that persists millennial microbial decomposition declines sharply with depth, with a preferential consumption of oxygen-rich moieties (Leifeld *et al.,* 2012). Hence, a higher PyC content in deeper peat may indicate selective enrichment of this material, owing to its retarded decomposition during peat formation. After drainage, selective enrichment of recalcitrant PyC may continue further and enhance the PyC/SOC ratio in disturbed relative to intact profiles. Dilution of the old, PyC-rich peat with variable amounts of fresh plant assimilates (Bader *et al.,* 2017), and fire prevention may smear the PyC/SOC–age relationship at managed sites which may explain why the increase in PyC/SOC with age was less distinct in degraded sites. Second, part of PyC is mobile in the soil profile. In mineral soils, PyC content is often higher in deeper layers (Brodowski *et al.,* 2007), attributed to increased solubility upon PyC oxidation (Hockaday *et al.,* 2007) and downward transport of the material in dissolved but also particulate form (Rumpel *et al.,* 2015). PyC transport has also been suggested as an important mechanism for larger PyC contents in deeper layers of organic soils when drained (Leifeld *et al.,* 2011). Global PyC exports to the ocean account for approximately 10% of the total riverine dissolved export, underpinning PyC's potentially large mobility (Jaffé *et al.,* 2013). Finally, fire frequencies may have changed over time, and a warmer mid-Holocene climate may have promoted more frequent fires (Clear *et al.,* 2014) and thus PyC accrual (Franzen & Malmgren, 2012). Higher PyC contents in older peat layers may reflect that history. With the available data, we cannot say which role either of those three factors play for the PyC pattern we encountered in organic soils but presume that they act jointly.

Pyrogenic carbon stocks in the analyzed organic soils (all samples, 0 to max 2 m, mean depth 0·49 m) were on average 5·8 (±0·9) kg C m^{-2}. They exceeded those reported for mineral soils [e.g., 0·6 ± 0·3 kg C m^{-2} (Soucémarianadin *et al.,* 2015); 0·1–1·5 kg C m^{-2} (Glaser & Amelung, 2003); 0·014–0·02 kg C m^{-2} (Czimczik *et al.,* 2003)] by one to three orders of magnitude. The fraction of PyC in soil C found here is similar to that previously reported for mineral soils; hence, the high stocks were caused by the overall greater SOC storage in organic soils compared with mineral soils.

We approximated the PyC pool for northern peatlands by using discrete peatland inception ages and their distribution from Loisel *et al.,* (2014) and the herein identified PyC–age relationship. For the total northern peatland C stock of 436 Pg (Loisel *et al.,* 2014), we calculated a PyC pool of 62·3 (±21·8) Pg or 14·3 (±5·0)% of the peatland C. The average PyC content of 14·3% calculated for northern peatlands this way is slightly higher than in our direct measurements (13·5%) because carbon in northern peatlands (Loisel *et al.,* 2014) is on average older (4,252 years) than in our sample set (3,527 years). The amount of northern peatland PyC is within the same order of magnitude as the global PyC pool estimated previously for all mineral and organic soils (Bird *et al.,* 2015; Reisser *et al.,* 2016; Santín *et al.,* 2016). Our PyC estimate for northern peatlands is associated with some uncertainties: The significant linear relationship between peat age and PyC explains only 30% of the variability in % PyC. It is also not known whether the observed PyC increase with age holds true for a wider range of natural peatlands that were not covered by our data set. Yet our estimate is based on sound methodology and the most comprehensive one reported hitherto.

CONCLUSIONS

Organic soils of intact and degrading peatlands contain up to 50% of pyrogenic carbon. The ratio of PyC to SOC increases with peat age and is higher when the peatland is drained. This suggests that preferential accumulation of PyC during peat formation and, after drainage, during peat oxidation, is an important mechanism in the fire related carbon cycle. A novel methodology for classifying peatlands as either intact or degraded proved reasonable and distinguished peat of systematically different chemical composition. Our estimate points to a potentially very high PyC stock in northern peatlands comparable with the present global soil PyC estimate. We therefore conclude that contemporary global soil PyC stock estimates require upward revision.

ACKNOWLEDGEMENTS

Robin Giger is acknowledged for analyzing elemental contents of all peat samples. Kari Minkkinen provided access to the Finnish sites. Andreas Grünig, Moritz Müller and Peter Trachsel helped in identifying appropriate sites in Switzerland. Edith Vogel assisted with the radiocarbon analysis. Part of the study was funded by the Swiss National Science Foundation, project number 200021_137569. This paper is dedicated to the the memory of Jon Lord, who passed away in 2012.

REFERENCES

Almendros G, Knicker H, González-Vila FJ. 2003. Rearrangement of carbon and nitrogen forms in peat after progressive thermal oxidation as determined by solid-state ^{13}C- and ^{15}N-NMR spectroscopy. *Organic Geochemistry* **34**: 1559–1568 https://doi.org/10.1016/S0146-6380.03.00152-9.

Bader C, Müller M, Schulin R, Leifeld J. 2017. Amount and stability of recent and aged plant residues in degrading peatland soils. *Soil Biology and Biochemistry* **109**: 167–175 https://doi.org/10.1016/j.soilbio.2017.01.029.

Baldock JA, Masiello CA, Gélinas Y, Hedges JI. 2004. Cycling and composition of organic matter in terrestrial and marine ecosystems. *Marine Chemistry* **92**: 39–64 https://doi.org/10.1016/j.marchem.2004.06.016.

Belyea LR, Malmer N. 2004. Carbon sequestration in peatland: patterns and mechanisms of response to climate change. *Global Change Biology* **10**: 1043–1052 https://doi.org/10.1111/j.1365-2486.2004.00783.x.

Berglund O, Berglund K, Klemedtsson L. 2010. A lysimeter study on the effect of temperature on CO_2 emission from cultivated peat soils. *Geoderma* **154**: 211–218 https://doi.org/10.1016/j.geoderma.2008.09.007.

Biester H, Knorr KH, Schellekens J, Basler A, Hermanns YM. 2014. Comparison of different methods to determine the degree of peat decomposition in peat bogs. *Biogeosciences* **11**: 2691–2707 https://doi.org/10.5194/bg-11-2691-2014.

Bird MI, Wynn JG, Saiz G, Wurster CM, McBeath A. 2015. The pyrogenic carbon cycle. *Annual Review of Earth and Planetary Sciences* **43**: 273–298 https://doi.org/10.1146/annurev-earth-060614-105038.

Bowman D, Balch JK, Artaxo P, Bond WJ, Carlson JM, Cochrane MA, D'Antonio CM, DeFries RS, Doyle JC, Harrison SP, Johnston FH, Keeley JE, Krawchuk MA, Kull CA, Marston JB, Moritz MA, Prentice IC, Roos CI, Scott AC, Swetnam TW, van der Werf GR, Pyne SJ. 2009. Fire in the Earth System. *Science* **324**: 481–484.

Brodowski S, Amelung W, Haumaier L, Zech W. 2007. Black carbon contribution to stable humus in German arable soils. *Geoderma* **139**: 220–228 https://doi.org/10.1016/j.geoderma.2007.02.004.

Clear JL, Molinari C, Bradshaw RHW. 2014. Holocene fire in Fennoscandia and Denmark. *International Journal of Wildland Fire* **23**: 781–789 https://doi.org/10.1071/WF13188.

Clymo RS. 1984. The limits to peat bog growth. *Philosophical Transactions of the Royal Society of London. Series B, Biological Sciences* **303**: 605–654 https://doi.org/10.1098/rstb.1984.0002.

Clymo RS, Turunen J, Tolonen K. 1998. Carbon accumulation in peatland. *Oikos* **81**: 368–388 https://doi.org/10.2307/3547057.

Czimczik CI, Preston CM, Schmidt MWI, Schulze ED. 2003. How surface fire in Siberian scots pine forests affects soil organic carbon in the forest floor: stocks, molecular structure, and conversion to black carbon. *Global Biogeochemical Cycles* **17** article 1020. https://doi.org/10.1029/2002GB001956.

Druffel ERM. 2004. Comments on the importance of black carbon in the global carbon cycle. *Marine Chemistry* **92**: 197–200 https://doi.org/10.1016/j.marchem.2004.06.026.

Franzen LG, Malmgren BA. 2012. Microscopic charcoal and tar particles in peat: a 6,500-year record of palaeo-fires in southern Sweden. *Mires and Peat* **10**: article 01.

Glaser B, Amelung W. 2003. Pyrogenic carbon in native grassland soils along a climosequence in North America. *Global Biogeochemical Cycles* **17** article 1064. https://doi.org/10.1029/2002gb002019.

Glaser B, Lehmann J, Zech W. 2002. Ameliorating physical and chemical properties of highly weathered soils in the tropics with charcoal – a review. *Biology and Fertility of Soils* **35**: 219–230 https://doi.org/10.1007/s00374-002-0466-4.

Hardy B, Cornelis JT, Houben D, Leifeld J, Lambert R, Dufey JE. 2017. Evaluation of the long-term effect of biochar on properties of temperate agricultural soil at pre-industrial charcoal kiln sites in Wallonia, Belgium. *European Journal of Soil Science* **68**: 80–89 https://doi.org/10.1111/ejss.12395.

Hartman BE, Chen H, Hatcher PG. 2015. A non-thermogenic source of black carbon in peat and coal. *International Journal of Coal Geology* **144**: 15–22 https://doi.org/10.1016/j.coal.2015.03.011.

Hedges JI, Eglinton G, Hatcher PG, Kirchman DL, Arnosti C, Derenne S, Evershed RP, Kögel-Knabner I, De Leeuw JW, Littke R, Michaelis W, Rullkotter J. 2000. The molecularly-uncharacterized component of nonliving organic matter in natural environments. *Organic Geochemistry* **31**: 945–958 https://doi.org/10.1016/S0146-6380(00)00096-6.

Hockaday WC, Grannas AM, Kim S, Hatcher PG. 2007. The transformation and mobility of charcoal in a fire-impacted watershed. *Geochimica et Cosmochimica Acta* **71**: 3432–3445 https://doi.org/10.1016/j.gca.2007.02.023.

Hua Q, Barbetti M, Rakowski AZ. 2013. Atmospheric radiocarbon for the period 1950–2010. *Radiocarbon* **55**: 2059–2072 https://doi.org/10.2458/azu_js_rc.v55i2.16177.

Jaffé R, Ding Y, Niggemann J, Vähätalo AV, Stubbins A, Spencer RGM, Campbell J, Dittmar T. 2013. Global charcoal mobilization from soils via dissolution and riverine transport to the oceans. *Science* **340**: 345–347 https://doi.org/10.1126/science.1231476.

Janzen HH. 2004. Carbon cycling in earth systems – a soil science perspective. *Agriculture Ecosystems & Environment* **104**: 399–417 https://doi.org/10.1016/j.agee.2004.01.040.

Joosten H. 2010. *The global peatland CO_2 picture. Peatland status and drainage related emissions in all countries of the world*. Wetlands International: Ede, NL; 36.

Kane ES, Hockaday WC, Turetsky MR, Masiello CA, Valentine DW, Finney BP, Baldock JA. 2010. Topographic controls on black carbon accumulation in Alaskan black spruce forest soils: implications for organic matter dynamics. *Biogeochemistry* **100**: 39–56 https://doi.org/10.1007/s10533-009-9403-z.

Kasimir-Klemedtsson A, Klemedtsson L, Berglund K, Martikainen P, Silvola J, Oenema O. 1997. Greenhouse gas emissions from farmed organic soils: a review. *Soil Use and Management* **13**: 245–250 https://doi.org/10.1111/j.1475-2743.1997.tb00595.x.

Konecny K, Ballhorn U, Navratil P, Jubanski J, Page SE, Tansey K, Hooijer A, Vernimmen R, Siegert F. 2016. Variable carbon losses from recurrent fires in drained tropical peatlands. *Global Change Biology* **22**: 1469–1480 https://doi.org/10.1111/gcb.13186.

Konovalov IB, Beekmann M, Kuznetsova IN, Yurova A, Zvyagintsev AM. 2011. Atmospheric impacts of the 2010 Russian wildfires: integrating modelling and measurements of an extreme air pollution episode in the Moscow region. *Atmospheric Chemistry and Physics* **11**: 10031–10056.

Krüger JP, Alewell C, Minkkinen K, Szidat S, Leifeld J. 2016. Calculating carbon changes in peat soils drained for forestry with four different profile-based methods. *Forest Ecology and Management* **381**: 29–36 https://doi.org/10.1016/j.foreco.2016.09.006.

Krüger JP, Leifeld J, Glatzel S, Szidat S, Alewell C. 2015. Biogeochemical indicators of peatland degradation – a case study of a temperate bog in northern Germany. *Biogeosciences* **12**: 2861–2871 https://doi.org/10.5194/bg-12-2861-2015.

Lehmann J, Skjemstad J, Sohi S, Carter J, Barson M, Falloon P, Coleman K, Woodbury P, Krull E. 2008. Australian climate–carbon cycle feedback reduced by soil black carbon. *Nature Geoscience* **1**: 832–835 https://doi.org/10.1038/ngeo358.

Leifeld J, Müller M, Fuhrer J. 2011. Peatland subsidence and carbon loss from drained temperate fens. *Soil Use and Management* **27**: 170–176 https://doi.org/10.1111/j.1475-2743.2011.00327.x.

Leifeld J, Steffens M, Galego-Sala A. 2012. Sensitivity of peatland carbon loss to organic matter quality. *Geophysical Research Letters* **39** article L14704. https://doi.org/10.1029/2012gl051856.

Liang B, Lehmann J, Solomon D, Sohi S, Thies JE, Skjemstad JO, Luizao FJ, Engelhard MH, Neves EG, Wirick S. 2008. Stability of biomass-derived black carbon in soils. *Geochimica et Cosmochimica Acta* **72**: 6069–6078 https://doi.org/10.1016/j.gca.2008.09.028.

Loisel J, Yu Z, Beilman DW, Camill P, Alm J, Amesbury MJ, Anderson D, Andersson S, Bochicchio C, Barber K, Belyea LR, Bunbury J, Chambers FM, Charman DJ, De Vleeschouwer F, Fiałkiewicz-Kozieł B, Finkelstein SA, Gałka M, Garneau M, Hammarlund D, Hinchcliffe W, Holmquist J, Hughes P, Jones MC, Klein ES, Kokfelt U, Korhola A, Kuhry P, Lamarre A, Lamentowicz M, Large D, Lavoie M, MacDonald G, Magnan G, Mäkilä M, Mallon G, Mathijssen P, Mauquoy D, McCarroll J, Moore TR, Nichols J, O'Reilly B, Oksanen P, Packalen M, Peteet D, Richard PJH, Robinson S, Ronkainen T, Rundgren M, Sannel ABK, Tarnocai C, Thom T, Tuittila ES, Turetsky M, Väliranta M, van der Linden M, van Geel B, van Bellen S, Vitt D, Zhao Y, Zhou W. 2014. A database and synthesis of northern peatland soil properties and Holocene carbon and nitrogen accumulation. *Holocene* **24**: 1028–1042 https://doi.org/10.1177/0959683614538073.

Pitkänen A, Grönlund E. 2001. A 600-year forest fire record in a varved lake sediment (Ristijärvi, Northern Karelia, Eastern Finland). *Annales Botanici Fennici* **38**: 63–73.

Ramsey CB. 2009. Bayesian analysis of radiocarbon dates. *Radiocarbon* **51**: 337–360 https://doi.org/10.2458/azu_js_rc.51.3494.

Reimer PJ, Bard E, Bayliss A, Beck JW, Blackwell PG, Ramsey CB, Buck CE, Cheng H, Edwards RL, Friedrich M, Grootes PM, Guilderson TP, Haflidason H, Hajdas I, Hatte C, Heaton TJ, Hoffmann DL, Hogg AG, Hughen KA, Kaiser KF, Kromer B, Manning SW, Niu M, Reimer RW, Richards DA, Scott EM, Southon JR, Staff RA, Turney CSM, van der Plicht J. 2013. INTCAL13 and MARINE13 radiocarbon age calibration curves 0–50,000 years cal BP. *Radiocarbon* **55**: 1869–1887 https://doi.org/10.2458/azu_js_rc.55.16947.

Rein G, Cleaver N, Ashton C, Pironi P, Torero JL. 2008. The severity of smouldering peat fires and damage to the forest soil. *Catena* **74**: 304–309 https://doi.org/10.1016/j.catena.2008.05.008.

Reisser M, Purves RS, Schmidt MWI, Abiven S. 2016. Pyrogenic carbon in soils: a literature-based inventory and a global estimation of its content in soil organic carbon and stocks. *Frontiers in Earth Science* **4** article 80. https://doi.org/10.3389/feart.2016.00080.

Rius D, Vanniere B, Galop D. 2009. Fire frequency and landscape management in the northwestern Pyrenean piedmont, France, since the early Neolithic (8000 cal. BP). *Holocene* **19**: 847–859 https://doi.org/10.1177/0959683609105299.

Rumpel C, Leifeld J, Santin C, Doerr S. 2015. In *Movement of biochar in the environment. Biochar for environmental management: science, technology and implementation*, Lehmann J, Joseph S (eds). Routledge, Taylor & Francis Group: Routledge, New York; 283–299.

Santín C, Doerr SH. 2016. Fire effects on soils: the human dimension. *Philosophical Transactions of the Royal Society, B: Biological Sciences* **371** article 20150171. https://doi.org/10.1098/rstb.2015.0171.

Santín C, Doerr SH, Kane ES, Masiello CA, Ohlson M, de la Rosa JM, Preston CM, Dittmar T. 2016. Towards a global assessment of pyrogenic carbon from vegetation fires. *Global Change Biology* **22**: 76–91 https://doi.org/10.1111/gcb.12985.

Scharlemann JPW, Tanner EVJ, Hiederer R, Kapos V. 2014. Global soil carbon: understanding and managing the largest terrestrial carbon pool. *Carbon Management* **5**: 81–91 https://doi.org/10.4155/cmt.13.77.

Sillasoo Ü, Väliranta M, Tuittila E-S. 2011. Fire history and vegetation recovery in two raised bogs at the Baltic Sea. *Journal of Vegetation Science* **22**: 1084–1093 https://doi.org/10.1111/j.1654-1103.2011.01307.x.

Skjemstad JO, Reicosky DC, Wilts AR, Mcgowan JA. 2002. Charcoal carbon in US agricultural soils. *Soil Science Society of America Journal* **66**: 1249–1255 https://doi.org/10.2136/sssaj2002.1249.

Smernik RJ, Schwark L, Schmidt MWI. 2006. Assessing the quantitative reliability of solid-state ^{13}C NMR spectra of kerogens across a gradient of thermal maturity. *Solid State Nuclear Magnetic Resonance* **29**: 312–321 https://doi.org/10.1016/j.ssnmr.2005.10.014.

Soucémarianadin LN, Quideau SA, MacKenzie MD, Munson AD, Boiffin J, Bernard GM, Wasylishen RE. 2015. Total and pyrogenic carbon stocks in black spruce forest floors from eastern Canada. *Organic Geochemistry* **82**: 1–11 https://doi.org/10.1016/j.orggeochem.2015.02.004.

Szidat S, Salazar GA, Vogel E, Battaglia M, Wacker L, Synal HA, Türler A. 2014. ^{14}C analysis and sample preparation at the New Bern Laboratory for the analysis of radiocarbon with AMS (LARA). *Radiocarbon* **56**: 561–566 https://doi.org/10.2458/56.17457.

Tolonen M. 1985. Palaeoecological record of local fire history from a peat deposit in SW Finland. *Annales Botanici Fennici* **22**: 15–29.

Turetsky MR, Benscoter B, Page S, Rein G, van der Werf GR, Watts A. 2015. Global vulnerability of peatlands to fire and carbon loss. *Nature Geoscience* **8**: 11–14.

Woolf D, Lehmann J. 2012. Modelling the long-term response to positive and negative priming of soil organic carbon by black carbon. *Biogeochemistry* **111**: 83–95 https://doi.org/10.1007/s10533-012-9764-6.

Wu M, Yang M, Han X, Zhong T, Zheng Y, Ding P, Wu W. 2015. Highly stable rice-straw-derived charcoal in 3,700-year-old ancient paddy soil: evidence for an effective pathway toward carbon sequestration. *Environmental Science and Pollution Research* **23**: 1007–1014 https://doi.org/10.1007/s11356-015-4422-x.

Yokelson RJ, Susott R, Ward DE, Reardon J, Griffith DWT. 1997. Emissions from smoldering combustion of biomass measured by open-path Fourier transform infrared spectroscopy. *Journal of Geophysical Research: Atmospheres* **102**: 18865–18877 https://doi.org/10.1029/97JD00852.

Yu ZC, Loisel J, Brosseau DP, Beilman DW, Hunt SJ. 2010. Global peatland dynamics since the last glacial maximum. *Geophysical Research Letters* **37** article L13402. https://doi.org/10.1029/2010gl043584.

Zaccone C, Rein G, D'Orazio V, Hadden RM, Belcher CM, Miano TM. 2014. Smouldering fire signatures in peat and their implications for palaeoenvironmental reconstructions. *Geochimica et Cosmochimica Acta* **137**: 134–146 https://doi.org/10.1016/j.gca.2014.04.018.

SUPPORTING INFORMATION

Additional Supporting Information may be found online in the supporting information tab for this article.

Fig. S1. Four ^{13}C NMR regions of 70 peat samples and their prediction by the molecular mixing model. Predicted = 1.088 (±0.094) + 0957 (±0.003) * x.

Fig. S2. Scores of the first two factors of principal component analysis of peat chemical composition. Open symbols represent degraded, filled symbols intact sites.

Fig. S3. van Krevelen diagram of studied peat samples.

Fig. S4. SEM–EDX images of four selected samples peat samples.

Fig. S5. Increase in carbon age with soil depth for intact and degraded sites.

Fig. S6. Increase in PyC/SOC ratios in four peat profiles. Table S1 shows the slope of the linear regressions and their statistical indices.

Table S1. Results from the linear regression analyses of PyC/SOC ratios in the four peat profiles shown in Figure S1.

